THE JOURNAL OF PHYSICAL CHEMISTRY Letters

pubs.acs.org/JPCL Letter

High-Resolution NMR of $S = 3/2$ Quadrupole Nuclei by Detection of Double-Quantum Satellite Transitions via Protons

Ivan Hung and Zhehong Gan*

Cite This: J. Phys. Chem. Lett. 2020, 11, 4734−4740 Read Online

ACCESS | Metrics & More | Article Recommendations

ABSTRACT: Indirect NMR detection via protons under fast magic-angle spinning can help overcome the low sensitivity and resolution of low-γ quadrupole nuclei such as ^{35}Cl. A robust and efficient method is presented for indirectly acquiring the double-quantum satellite-transition (DQ-ST) spectra of quadrupole nuclei. For a spin $S = 3/2$, the DQ-STs have a much smaller second-order quadrupolar broadening, one-ninth compared to that of the central transition. Thus, they can provide a factor of up to 18 in resolution enhancement. The indirect detection of DQ-STs via protons is carried out using the heteronuclear multiple-quantum coherence (HMQC) experiment with the transfer of populations in double-resonance (TRAPDOR) recoupling mechanism. The resolution enhancement by detecting DQ-STs and the high efficiency of the TRAPDOR-HMQC experiment are demonstrated by ^{35}Cl NMR of several active pharmaceutical ingredients (APIs).

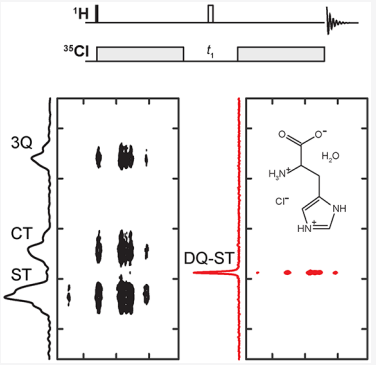

The majority of elements in the periodic table have a nuclear spin $S > 1/2$ and thus possess quadrupole couplings. Many of them have large quadrupole moments and low gyromagnetic ratios γ, like ^{25}Mg, ^{35}Cl, ^{39}K, ^{43}Ca, ^{47,49}Ti, ^{61}Ni, ^{67}Zn, ^{73}Ge, ^{91}Zr, and ^{99}Ru, making their NMR spectral acquisition difficult. Indirect detection via sensitive spin $S = 1/2$ nuclei, especially the highly abundant protons, can help overcome the low resolution and sensitivity problems. In addition, heteronuclear correlation provides structural and spatial proximity information useful for the characterization of a variety of materials including metal−organic frameworks (MOFs), catalysis, battery electrode and ionic conductor materials, proteins, and pharmaceuticals. In the solid-state, cross-polarization (CP) is the most common method for establishing heteronuclear correlation and indirect detection.[1,2] However, for quadrupole nuclei, methods using the hetero-nuclear multiple-quantum coherence (HMQC)[3−7] and in-sensitive nuclei enhanced by polarization transfer (INEPT)[8,9] are preferred, because CP has the issue of maintaining spin-lock with quadrupolar nuclei under magic-angle spinning (MAS) due to their multiple transitions and large frequency offsets.[10,11] The HMQC sequence in particular requires only a pair of pulses applied to the indirectly detected nucleus and can thus be adapted more easily to correlating transitions like satellite, multiple-quantum, or even overtone transitions.[6,7,12] Improving the efficiency for polarization transfer or creation of heteronuclear coherences is of key importance to indirect detection experiments, especially for low-γ nuclei that have low natural abundance and/or weak dipolar couplings. When the efficiency is low, t_1 noise can overwhelm two-dimensional experiments. Methods using various types of recoupling[13−15] and purging of unwanted signals[16,17] have been developed to address the efficiency and t_1-noise problems.

The second-order quadrupolar broadening remains under MAS, often preventing site resolution. Although high magnetic fields can help reduce the second-order effect,[18,19] only 2D experiments like multiple-quantum magic-angle spinning (MQMAS) ultimately allow isotropic spectral resolution to be obtained in a practical manner.[20] The MQMAS method and its variant satellite-transition magic-angle spinning (STMAS)[21] have been incorporated into the indirect detection experiments such that isotropic spectra without anisotropic broadening can be obtained along the indirect dimension.[22−30] While superior in terms of spectral resolution, the implementation of MQMAS or STMAS is often limited by low efficiency especially for low-γ nuclei. Indeed, the efficiency for excitation and conversion of multiple-quantum coherences are often low due to insufficient *rf* fields $\omega_1 = -\gamma B_1$ as compared to the large quadrupole couplings.[31] For indirectly detected MQMAS experiments, the low efficiency for indirect detection compounds that of MQMAS, making the sensitivity problem even worse. In this work, we present a novel proton-detected NMR experiment that addresses the resolution and efficiency in a different way. The proposed HMQC experiment correlates in one step with

Received: April 22, 2020
Accepted: May 26, 2020
Published: May 27, 2020

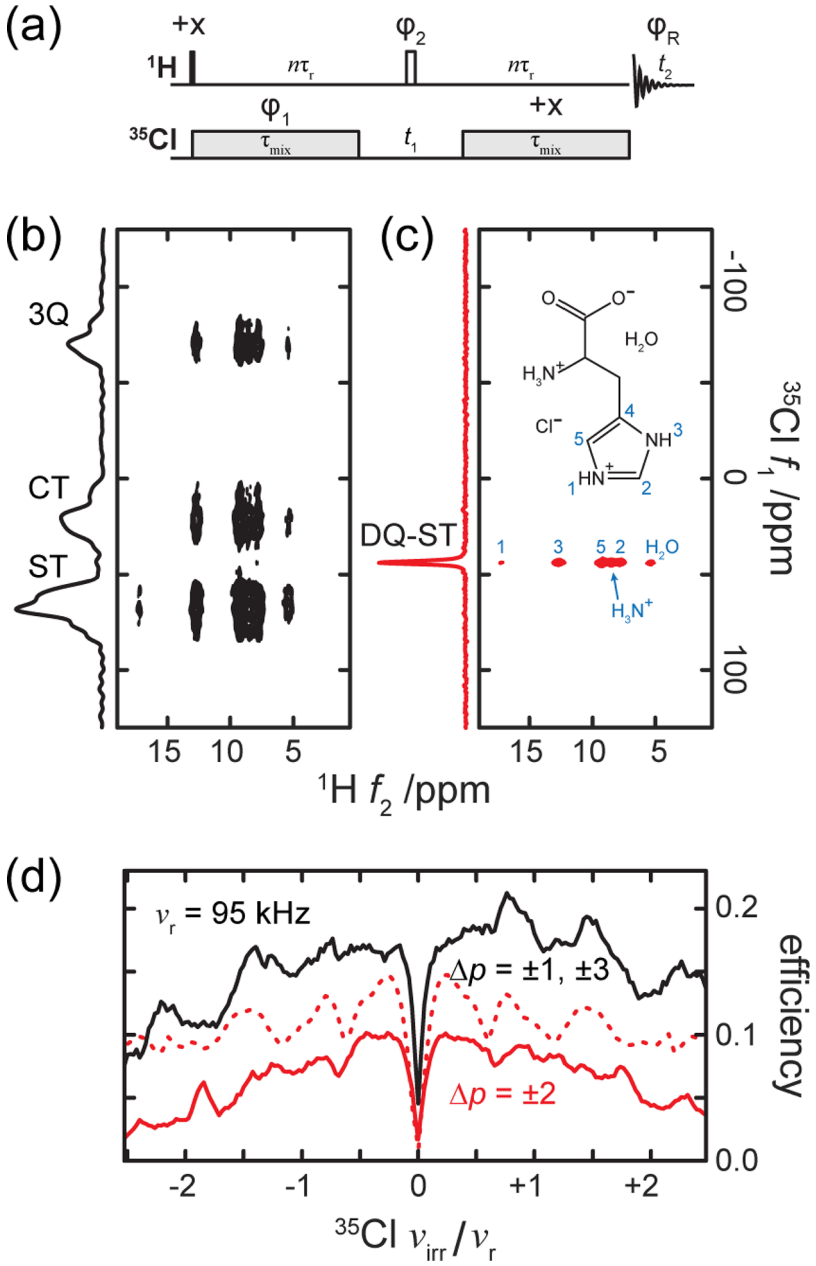

Figure 1. (a) Schematic of the T-HMQC pulse sequence. $^{1}H/^{35}Cl$ T-HMQC spectra of histidine·HCl·H_2O acquired by selecting the ^{35}Cl (b) single- and triple-quantum, or (c) only the double-quantum coherences during t_1. (d) Frequency profiles of the experimental (solid lines) and simulated (dashed line) efficiencies for the experiments in (b) in black and (c) in red as compared to the intensity of a ^{1}H spin−echo. The DQ-ST simulation is plotted without taking into account the 75.8% natural abundance of ^{35}Cl nuclei. 2D spectra were acquired with ν_r = 95 kHz MAS, 18.8 T field, $\tau_{mix} \sim$ 1.7 ms, t_1 dwell of $2/\nu_r$, 8 transients per t_1 increment, 95 and 256 complex t_1 points, and 51 and 137 min total acquisition time for the $\Delta p = \pm 1, \pm 3$ and $\Delta p = \pm 2$ experiments, respectively. The base contours for the 2D spectra were set at 6% of the maximum intensity. The phase cycle used to select the ^{35}Cl $\Delta p = \pm 1, \pm 3$ coherence transfer pathways is $\{\varphi_1 = 02; \varphi_2 = 00\ 11\ 22\ 33; \varphi_R = 02\ 20\}$, and for $\Delta p = \pm 2$ it is $\{\varphi_1 = 0123; \varphi_2 = 0000\ 1111\ 2222\ 3333; \varphi_R = 0202\ 2020\}$, where 0, 1, 2, and 3 are 90° multiples of the phase. Simulation of the DQ-ST frequency profile in (d) was performed using SIMPSON[41] for a single $^{1}H-^{35}Cl$ spin pair with dipole coupling of −580 Hz, and ^{35}Cl C_Q = 1.95 MHz, η_Q = 0.66.[16] All other simulation parameters were set to match experimental values.

the double-quantum satellite-transitions (DQ-STs) directly. For spin $S = 3/2$ quadrupole nuclei, it will be shown that the DQ-ST MAS spectra are nearly isotropic, and thus, high spectral resolution can be obtained without going through excitation and conversion of multiple-quantum coherences.

The high efficiency and spectral resolution of the DQ-ST HMQC experiment will be demonstrated by the proton-detected ^{35}Cl NMR spectra of several hydrochloride salts of pharmaceutical compounds. More than 50% of active pharmaceutical ingredients (APIs) are produced as HCl salts. ^{35}Cl NMR enables the measurement of chemical shift and electric field gradient (EFG) parameters that are sensitive to the local structure around the chlorine sites, such as the hydrogen bonding environment.[32,33] With the aid of density functional theory (DFT) calculations, information can be obtained about structure and polymorphism, which are important to the physicochemical and pharmacokinetic properties of APIs.[34,35] Even when using high magnetic fields,

https://dx.doi.org/10.1021/acs.jpclett.0c01236
J. Phys. Chem. Lett. 2020, 11, 4734−4740

^{35}Cl NMR of APIs can be challenging due to large quadrupolar broadening. The high spectral resolution obtained here by detecting the DQ-STs can be useful to resolve overlapping ^{35}Cl sites and measure ^{35}Cl quadrupolar coupling parameters. Proton-detected ^{35}Cl NMR can also be used to filter out large ^{1}H background signals from excipients to obtain the ^{1}H signals of APIs next to ^{35}Cl sites. Although the usage of ^{1}H indirect detection and DQ-ST HMQC are demonstrated here with ^{35}Cl NMR of APIs, the presented method is applicable generally to spin $S = 3/2$ nuclei.

Experiments on histidine·HCl·H_2O were carried out at $\nu_0(^1H) = 800.1$ MHz and $\nu_0(^{35}Cl) = 78.4$ MHz using an 800 MHz Bruker Avance III HD spectrometer and a 0.75 mm MAS probe developed at the National High Magnetic Field Laboratory (NHMFL) using a spinning assembly and rotors from JEOL. The 0.75 mm rotor holds approximately 290 nL of histidine·HCl·H_2O, and a spinning frequency of 95 kHz was used for measurements. The spinning speed was regulated to within ±5 Hz, and the recycle delay was 2 s. The magic-angle setting was calibrated directly on the histidine sample by narrowing the ^{35}Cl DQ-ST line width along the indirection dimension of a 2D ^{1}H/^{35}Cl TRAPDOR-HMQC spectrum. Experiments on the API samples were performed with Bruker 1.3 mm MAS probes spinning at 60 kHz. Spectra acquired at 14.1 T were carried out at $\nu_0(^1H) = 600.1$ MHz and $\nu_0(^{35}Cl) = 58.8$ MHz using a Bruker Avance NEO spectrometer. Recycle delays of 3 and 4 s were used for the diphenhydramine and isoxsuprine samples, respectively. The approximate ^{35}Cl *rf* fields used were 85 kHz on the 800 0.75 mm probe, 100 kHz on the 800 1.3 mm probe, and 140 kHz on the 600 1.3 mm probe. Other relevant experimental parameters are included in the figure captions.

The pulse sequence used to acquire ^{1}H/^{35}Cl HMQC spectra is shown in Figure 1a. The long pulses applied on the ^{35}Cl nuclei reintroduce the heteronuclear dipolar coupling through the TRAnsfer of Populations in DOuble-Resonance (TRAPDOR) mechanism,[36−38] which has previously been used for HMQC detection of ^{14}N, the spin $S = 1$ isotope of nitrogen.[39,40] For satellite transitions (STs) with frequency spans far larger than the *rf* field strength, MAS causes brief level crossings between the *rf* and ST frequencies during a rotor period. Thus, the level crossings induce periodic perturbation among the spin states, or transfer of population. These periodic perturbations disrupt the averaging of the spatial component of the dipolar coupling, reintroducing the interaction under MAS. TRAPDOR recoupling is simple and robust, but it is difficult to obtain an analytical solution for the recoupling mechanism due to the complexity of the spin dynamics.[36−38] Numerical simulations are often required for analysis and interpretation. Here, the SIMPSON program[41] is used to simulate the HMQC experiment using TRAPDOR recoupling.

The pair of long pulses in the HMQC sequence also serve to encode the ^{35}Cl frequency. Phase cycling of the two pulses can select the change in coherence order Δp for the various transitions within the spin $S = 3/2$ ^{35}Cl nucleus.[42,43] The two-step phase cycle typically used for the indirectly detected channel in HMQC experiments of $S = 1/2$ nuclei selects the single-quantum (SQ) coherences of the central transition *and* the pair of STs when applied to $S = 3/2$ nuclei. The ^{1}H/^{35}Cl TRAPDOR-HMQC, or T-HMQC, spectrum of histidine·HCl·H_2O using such phase cycling is shown in Figure 1b. The pair of STs appear as a single peak when the first-order quadrupolar coupling is averaged by spinning accurately at the magic-angle and by synchronizing the t_1 evolution time with the spinning frequency. In addition to the CT and ST resonances, it was puzzling to observe the appearance of a third peak, which did not maintain the same relative position to the other two peaks when changing the transmitter frequency. It was eventually realized that the extraneous peak comes from the triple-quantum (3Q) coherence, since a two-step phase cycle that selects $\Delta p = \pm 1$ also permits $\Delta p = \pm 3$.[42,43] All three signals (CT, ST, and 3Q) are broadened by the second-order quadrupole coupling along the indirect ^{35}Cl dimension of the 2D spectrum. Their relative integrated intensities correspond with the respective quantity of such transitions in $S = 3/2$ nuclei, i.e., the CT, ST, and 3Q peaks have a ratio of approximately 1:2:1 as seen in the f_1 projection. This observation indicates that the different coherences for the $S = 3/2$ spin build up at similar rates in the T-HMQC experiment, including the double-quantum satellite-transitions (DQ-STs). Efficient generation of such heteronuclear coherences is what eventually led us to exploit the unique spectral resolution of DQ-STs for spin $S = 3/2$ nuclei.

A four-step phase cycle of the indirectly detected channel in HMQC selects a change in coherence order of $\Delta p = \pm 2$. Using such a phase cycle for the ^{1}H/^{35}Cl T-HMQC spectrum of histidine·HCl·H_2O shows a much narrower peak for the pair of DQ-STs (Figure 1c). The DQ signals are concentrated into a narrow resonance giving a higher signal-to-noise ratio (S/N) compared to the other transitions. For half-integer quadrupole nuclei, the $l = 0$ isotropic and the $l = 4$ anisotropic terms of the second-order quadrupolar shift remain under MAS. The relative ratios among the various transitions have been derived.[20,44−46] Between the single-quantum transition $|m_s + 1/2> \leftrightarrow |m_s - 1/2>$ and the central transition (i.e., for $m_s = 0$), they are given by[44−46]

$$R^0_{S,m_S} = 1 - \frac{36m_S^2}{4S(S+1) - 3}, \quad R^4_{S,m_S} = 1 - \frac{68m_S^2}{3[4S(S+1) - 3]} \tag{1}$$

The ratios for the DQ-STs can be obtained from the sum of one ST and the CT (i.e., $R^l_{S,1} + R^l_{S,0}$). For spin $S = 3/2$

$$R^0_{3/2,DQ} = -1, \; R^4_{3/2,DQ} = 1/9 \tag{2}$$

Thus, the quadrupole broadening of the DQ-ST transitions $R^{l=4}_{3/2,DQ}$ is 1/9 compared to the CT, in units of frequency. Considering that the chemical shift separation for DQ transitions is twice that of SQ transitions in units of frequency, the final resolution enhancement by observing the DQ-STs over the CT can be up to a factor of 18 if the differences in T_2 relaxation and other contributions to line broadening are not considered. Therefore, observation of the DQ-STs for $S = 3/2$ nuclei provides better S/N *and* resolution than detection of any other transition. It is important to note that the DQ-STs are subject to the large first-order quadrupole coupling, which is only properly averaged when the sample spinning occurs very accurately at the "magic angle". Therefore, calibration of the magic angle is critical and needs to meet the same stringent requirement as for the STMAS experiment.[21]

Figure 1d shows the frequency offset profiles of T-HMQC normalized by the intensity of a ^{1}H spin−echo. The profiles for all quanta show a notch on-resonance, which agrees with simulations. When the *rf* is off-resonance with the CT, the level

https://dx.doi.org/10.1021/acs.jpclett.0c01236
J. Phys. Chem. Lett. 2020, 11, 4734−4740

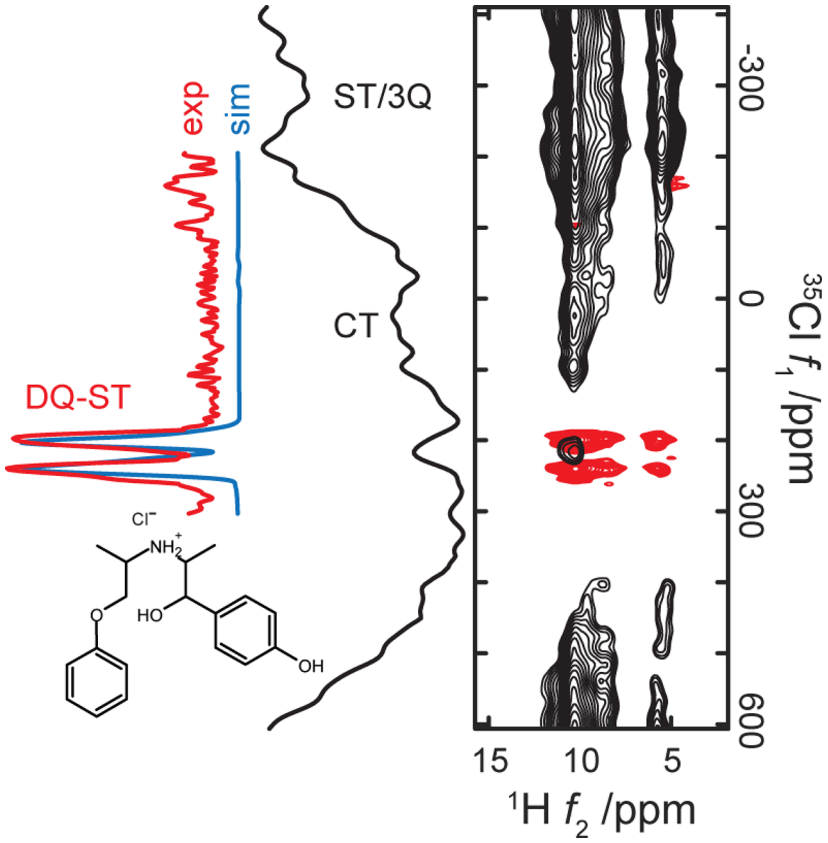

Figure 2. $^{1}H/^{35}Cl$ T-HMQC spectra of an isoxsuprine·HCl polymorph (Isox-II) in bulk form, comparing the DQ-ST (red) and other ^{35}Cl transitions (black) spectra acquired with ν_r = 60 kHz MAS, 14.1 T field, τ_{mix} = 0.6 ms, t_1 dwell of $1/\nu_r$, 128 transients per t_1 increment, 32 and 45 complex t_1 points, and 9.1 and 12.8 h total acquisition times for the $\Delta p = \pm 1, \pm 3$ and $\Delta p = \pm 2$ experiments, respectively. The base contours for the 2D spectra were set at 20% of the maximum intensity.

crossings for the pair STs with the *rf* occur sequentially. However, for on-resonance *rf* pulses, the crossings occur at the same time for the pair of STs and the CT, inducing transfers among all four levels simultaneously. This difference is likely the cause for the on-resonance notch. Hence, the T-HMQC experiment should be carried out with the ^{35}Cl transmitter frequency near one of the first spinning sideband positions in order to avoid the notch. With a rotor-synchronized t_1 evolution time, the DQ-ST peaks can be made to appear at the same position as with an on-resonance transmitter frequency by changing the chemical shift reference frequency by the same amount as done for the transmitter frequency.[40] The overall DQ efficiency is relatively high at ∼10%, considering the weak dipolar couplings from the protons to the nondirectly bonded low-γ nuclei (r_{H-Cl} > 2.0 Å) and the 75.8% natural abundance of ^{35}Cl. By comparison, the direct HMQC correlation to the DQ-STs is much more efficient than other D-HMQC methods combined with MQMAS or STMAS for obtaining isotropic resolution.[28,29] The high efficiency and robust TRAPDOR recoupling also make T-HMQC less susceptible to t_1 noise compared to other methods that apply dipolar recoupling to the observe channel.[40]

The application of ^{35}Cl NMR to active pharmaceutical ingredients (APIs) faces several challenges. Even at high magnetic fields, the ^{35}Cl quadrupolar broadening often remains large, preventing site resolution for APIs with multiple chlorine sites. Deconvolution of quadrupolar line shapes is often used, provided there are sufficient spectral features and signal-to-noise, to extract chemical shift and EFG parameters as exemplified for the isoxsuprine·HCl polymorph (Isox-II) in ref 33. Figure 2 demonstrates the ^{35}Cl resolution enhancement obtained in the proton-detected DQ-ST T-HMQC experiment. The ^{35}Cl quadrupole couplings in Isox-II are larger than for histidine·HCl·H_2O. The CT, ST, and 3Q signals overlap beyond identification and are almost as broad as the rotor-synchronized f_1 spectral window of 60 kHz. On the other hand, the DQ-ST spectrum shows two completely resolved peaks from the two crystallographic inequivalent chlorine sites. The peak positions and line widths agree well with a simulation using the chemical shift and quadrupolar coupling parameters reported in the literature (δ_{iso} = 130 ppm, C_Q = 6.4 MHz, η_Q = 0.33; δ_{iso} = 125 ppm, C_Q = 5.7 MHz, η_Q = 0.31).[33] It should be noted that when comparing SQ and DQ spectra, the spectral window is halved in the ppm scale due to doubling of the Larmor frequency for DQ transitions. Here the "unified" ppm scale definition used for MQMAS and STMAS spectra is adopted,[45] which is different from the ppm axis commonly used for two-spin DQ spectra.

The line narrowing obtained by acquiring ^{35}Cl DQ-ST spectra enables more easily the measurement of the isotropic quadrupolar shift, which in turn allows determination of the quadrupolar coupling parameter P_Q without the need for line shape fitting. Figure 3a compares $^{1}H/^{35}Cl$ DQ-ST T-HMQC spectra of diphenhydramine·HCl acquired at two magnetic fields. The ^{35}Cl DQ-ST peak appears at $\delta^{DQ\text{-}ST}$ = 132.4 and 100.0 ppm for 14.1 and 18.8 T, respectively. The shift difference arises from the inverse square dependence of the isotropic second-order quadrupole shift, in units of frequency,

https://dx.doi.org/10.1021/acs.jpclett.0c01236
J. Phys. Chem. Lett. 2020, 11, 4734−4740

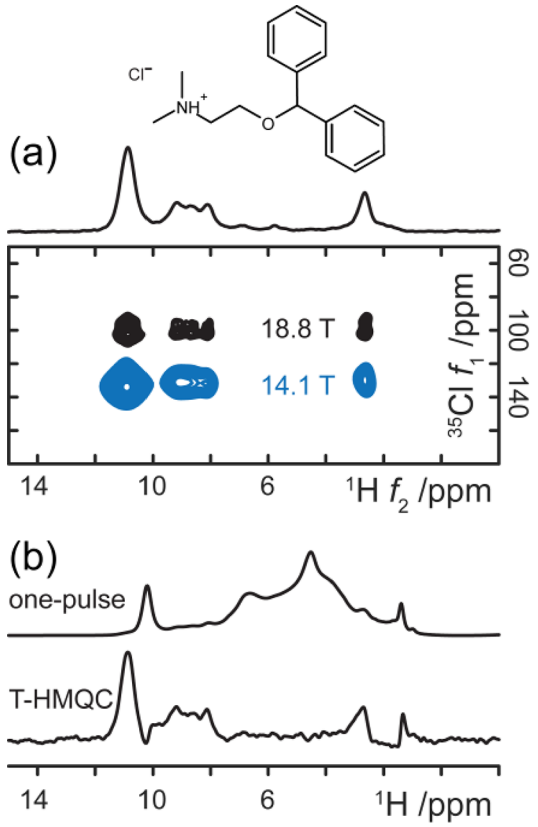

Figure 3. (a) ^{1}H/^{35}Cl DQ-ST T-HMQC spectra of diphenhydramine·HCl in bulk form acquired at 60 kHz MAS, and τ_{mix} = 0.6 ms at 14.1 T and 0.8 ms at 18.8 T. Acquisition of the 2D spectra used a t_1 dwell of $1/\nu_r$, 128 transients per t_1 increment, 32 and 60 complex t_1 points, and total acquisition times of 6.8 and 12.8 h, respectively, for the 14.1 and 18.8 T experiments. The base contours for the 2D spectra were set at 15% of the maximum intensity and the sum projection for the 18.8 T spectrum is shown on top. (b) Comparison of ^{1}H spectra between one-pulse excitation and the first T-HMQC ($\Delta p = \pm 1, \pm 3$) t_1 increment acquired at 18.8 T of diphenhydramine·HCl in dosage form. The T-HMQC filters out ^{1}H signals from the excipients and shows the ^{1}H signals in proximity to ^{35}Cl sites of the API (~6% wt in the dosage form).

on the magnetic field. For the CT, the isotropic quadrupolar induced shift (QIS) in units of ppm is

$$\delta_{QIS} = \frac{P_Q^2}{\nu_0^2} \cdot \frac{3\left[\frac{3}{4} - S(S+1)\right]}{10[2S(2S-1)]^2} \cdot 10^6 \quad (3)$$

Eq 2 implies that the shift of the DQ-ST peak in units of ppm, after dividing by twice the Larmor frequency, is given by

$$\delta^{DQST} = \delta_{iso} - \delta_{QIS}/2 \quad (4)$$

By measuring δ^{DQST} at two different fields, the isotropic chemical (δ_{iso}) and quadrupole (δ_{QIS}) shifts can be separated and determined. The magnitude of the quadrupole coupling $P_Q = C_Q\,(1 + \eta_Q^2/3)$ can be then obtained directly from the δ_{QIS} without simulation and/or fitting of the line shape. In the case of diphenhydramine·HCl, the difference in δ^{DQST} between the two fields is 32.4 ppm, which yields an isotropic chemical shift of δ_{iso} = 58.4 ppm and P_Q = 4.5 MHz. These values are in good agreement with the δ_{iso} = 51 ppm and P_Q = 4.55 MHz values obtained in the literature by line shape fitting.[33]

It is often desirable to acquire and separate the proton signals of diluted APIs in the dosage form from the strong background signals of excipients in order to monitor the effects of tablet preparation on APIs. The task can be challenging due to insufficient proton spectral resolution to distinguish API signals from those of excipients. The use of hydrochloride salts in more than 50% of APIs offers a possibility to use ^{35}Cl filtering to identify the proton signals based on their proximity to ^{35}Cl sites. Figure 3b compares a 1D ^{1}H/^{35}Cl T-HMQC spectrum at t_1 = 0 for diphenhydramine·HCl in the pill form with its ^{1}H one-pulse excitation spectrum. The comparison shows the filtration of ^{1}H signals that are distant from ^{35}Cl sites in the API. The filtered HMQC spectrum from the dosage form agrees well with the spectrum from the bulk form in Figure 3a. Some artifacts remain due to incomplete subtraction of the strong and sharp signals from the excipients, e.g., at ~1.5 ppm. It should be noted that the API proton signals are very small in the one-pulse spectrum, hidden beneath those of the excipients. The HMQC filtered signal is less than 1% compared to the direct excitation spectrum as estimated from the ~6 wt % of API in the dosage form[33] and the efficiency of the ^{1}H/^{35}Cl T-HMQC experiment measured from the model compounds in Figure 1. Nevertheless, the large background signals are largely subtracted out by HMQC filtering.

The proton-detected T-HMQC experiment benefits from high magnetic fields and fast MAS. Besides increasing ^{1}H signal intensity, higher B_0 fields also improve proton resolution and reduce ^{35}Cl line broadening caused by the second-order quadrupole interaction, thus improving the resolution along both dimensions. Fast magic-angle spinning also helps the T-HMQC experiment in multiple ways by improving ^{1}H resolution, lengthening ^{1}H T_2 relaxation and increasing the rotor-synchronized indirect dimension spectral window. A larger spectral window along the ^{35}Cl dimension helps to accommodate signals with large quadrupole couplings and/or broadening. The T-HMQC experiment benefits particularly from long ^{1}H T_2 values under fast MAS given the relatively long ^{1}H spin−echo used in the pulse sequence.

In summary, it has been shown that indirect proton detection under fast MAS can acquire spectra of the various transitions in quadrupole nuclei efficiently using the T-HMQC pulse sequence. For S = 3/2 nuclei such as ^{35}Cl, the double-quantum satellite transitions have one-ninth of the quadrupolar broadening as compared to the conventionally observed central transition and can thus offer up to a factor of 18 in resolution enhancement. The high efficiency and robustness of the T-HMQC experiment have been demonstrated with ^{35}Cl NMR of active pharmaceutical ingredients. The dramatic line narrowing obtained by observing the ^{35}Cl double-quantum satellite transitions achieves near isotropic resolution, which can help to resolve overlapping hydrochloride sites in APIs as well as measure the structurally informative chemical shift and electric field gradient parameters. The DQ-ST experiment does need a precise magic-angle setting to average out the large first-order quadrupolar broadening to the satellite transitions. Improved specifications in this regard for commercial NMR probes will facilitate applications not only to ^{35}Cl NMR but also other S = 3/2 nuclei in general, overcoming low sensitivity and resolution issues especially for low-γ nuclei.

https://dx.doi.org/10.1021/acs.jpclett.0c01236
J. Phys. Chem. Lett. 2020, 11, 4734−4740

AUTHOR INFORMATION

Corresponding Author

Zhehong Gan − *National High Magnetic Field Laboratory, Tallahassee, Florida 32310, United States;* orcid.org/0000-0002-9855-5113; Email: gan@magnet.fsu.edu; Fax: +1 850 644 1366

Author

Ivan Hung − *National High Magnetic Field Laboratory, Tallahassee, Florida 32310, United States*

Complete contact information is available at: https://pubs.acs.org/10.1021/acs.jpclett.0c01236

Notes

The authors declare no competing financial interest.

ACKNOWLEDGMENTS

This work was supported by the National High Magnetic Field Laboratory (NHMFL) through a National Science Foundation Cooperative Agreement (DMR-1644779) and by the State of Florida. API samples were kindly provided by Prof. R. W. Schurko. We thank Mr. P. L. Gor'kov, Mr. R. Desilets of the NHMFL, and Mr. Y. Endo, Mr. T. Nemoto, and Dr. Y. Nishiyama of JEOL for the development and construction of the 100 kHz MAS probe using a 0.75 mm spinning module.

REFERENCES

(1) Hartmann, S. R.; Hahn, E. L. Nuclear Double Resonance in Rotating Frame. *Phys. Rev.* **1962**, *128* (5), 2042−2053.

(2) Caravatti, P.; Bodenhausen, G.; Ernst, R. R. Heteronuclear Solid-State Correlation Spectroscopy. *Chem. Phys. Lett.* **1982**, *89* (5), 363−367.

(3) Muller, L. Sensitivity Enhanced Detection of Weak Nuclei Using Heteronuclear Multiple Quantum Coherence. *J. Am. Chem. Soc.* **1979**, *101* (16), 4481−4484.

(4) Minoretti, A.; Aue, W. P.; Reinhold, M.; Ernst, R. R. Coherence Transfer by Radiofrequency Pulses for Heteronuclear Detection of Multiple-Quantum Transitions. *J. Magn. Reson.* **1980**, *40* (1), 175−190.

(5) Iuga, D.; Morais, C.; Gan, Z.; Neuville, D. R.; Cormier, L.; Massiot, D. NMR Heteronuclear Correlation between Quadrupolar Nuclei in Solids. *J. Am. Chem. Soc.* **2005**, *127* (33), 11540−11541.

(6) Gan, Z. Measuring Amide Nitrogen Quadrupolar Coupling by High-Resolution N-14/C-13 NMR Correlation under Magic-Angle Spinning. *J. Am. Chem. Soc.* **2006**, *128* (18), 6040−6041.

(7) Cavadini, S.; Lupulescu, A.; Antonijevic, S.; Bodenhausen, G. Nitrogen-14 NMR Spectroscopy Using Residual Dipolar Splittings in Solids. *J. Am. Chem. Soc.* **2006**, *128* (24), 7706−7707.

(8) Morris, G. A.; Freeman, R. Enhancement of Nuclear Magnetic-Resonance Signals by Polarization Transfer. *J. Am. Chem. Soc.* **1979**, *101* (3), 760−762.

(9) Fyfe, C. A.; Wong-Moon, K. C.; Huang, Y.; Grondey, H. INEPT Experiments in Solid-State NMR. *J. Am. Chem. Soc.* **1995**, *117* (41), 10397−10398.

(10) Vega, A. J. MAS NMR Spin Locking of Half-Integer Quadrupolar Nuclei. *J. Magn. Reson.* **1992**, *96* (1), 50−68.

(11) Vega, A. J. CP/MAS of Quadrupolar S = 3/2 Nuclei. *Solid State Nucl. Magn. Reson.* **1992**, *1* (1), 17−32.

(12) Nishiyama, Y.; Malon, M.; Gan, Z. H.; Endo, Y.; Nemoto, T. Proton-Nitrogen-14 Overtone Two-Dimensional Correlation NMR Spectroscopy of Solid-Sample at Very Fast Magic Angle Sample Spinning. *J. Magn. Reson.* **2013**, *230*, 160−164.

(13) Oas, T. G.; Griffin, R. G.; Levitt, M. H. Rotary Resonance Recoupling of Dipolar Interactions in Solid-State Nuclear Magnetic-Resonance Spectroscopy. *J. Chem. Phys.* **1988**, *89* (2), 692−695.

(14) Brinkmann, A.; Kentgens, A. P. M. Proton-Selective O-17-H-1 Distance Measurements in Fast Magic-Angle-Spinning Solid-State NMR Spectroscopy for the Determination of Hydrogen Bond Lengths. *J. Am. Chem. Soc.* **2006**, *128* (46), 14758−14759.

(15) Lu, X.; Lafon, O.; Trébosc, J.; Tricot, G.; Delevoye, L.; Méar, F.; Montagne, L.; Amoureux, J. P. Observation of Proximities between Spin-1/2 and Quadrupolar Nuclei: Which Heteronuclear Dipolar Recoupling Method Is Preferable? *J. Chem. Phys.* **2012**, *137* (14), 144201.

(16) Venkatesh, A.; Hanrahan, M. P.; Rossini, A. J. Proton Detection of MAS Solid-State NMR Spectra of Half-Integer Quadrupolar Nuclei. *Solid State Nucl. Magn. Reson.* **2017**, *84*, 171−181.

(17) Perras, F. A.; Pruski, M. Reducing T1 Noise through Rapid Scanning. *J. Magn. Reson.* **2019**, *298*, 31−34.

(18) Gan, Z. H.; Gor'kov, P.; Cross, T. A.; Samoson, A.; Massiot, D. Seeking Higher Resolution and Sensitivity for NMR of Quadrupolar Nuclei at Ultrahigh Magnetic Fields. *J. Am. Chem. Soc.* **2002**, *124* (20), 5634−5635.

(19) Gan, Z.; Hung, I.; Wang, X. L.; Paulino, J.; Wu, G.; Litvak, I. M.; Gor'kov, P. L.; Brey, W. W.; Lendi, P.; Schiano, J. L.; Bird, M. D.; Dixon, L. R.; Toth, J.; Boebinger, G. S.; Cross, T. A. NMR Spectroscopy up to 35.2 T Using a Series-Connected Hybrid Magnet. *J. Magn. Reson.* **2017**, *284*, 125−136.

(20) Frydman, L.; Harwood, J. S. Isotropic Spectra of Half-Integer Quadrupolar Spins from Bidimensional Magic-Angle-Spinning NMR. *J. Am. Chem. Soc.* **1995**, *117* (19), 5367−5368.

(21) Gan, Z. H. Isotropic NMR Spectra of Half-Integer Quadrupolar Nuclei Using Satellite Transitions and Magic-Angle Spinning. *J. Am. Chem. Soc.* **2000**, *122* (13), 3242−3243.

(22) Wang, S. H.; De Paul, S. M.; Bull, L. M. High-Resolution Heteronuclear Correlation between Quadrupolar and Spin-1/2 Nuclei Using Multiple-Quantum Magic-Angle Spinning. *J. Magn. Reson.* **1997**, *125* (2), 364−368.

(23) Fernandez, C.; Morais, C.; Rocha, J.; Pruski, M. High-Resolution Heteronuclear Correlation Spectra between 31P and 27Al in Microporous Aluminophosphates. *Solid State Nucl. Magn. Reson.* **2002**, *21* (1−2), 61−70.

(24) Wiench, J. W.; Pruski, M. Probing through Bond Connectivities with MQMAS NMR. *Solid State Nucl. Magn. Reson.* **2004**, *26* (1), 51−55.

(25) Wiench, J. W.; Tricot, G.; Delevoye, L.; Trebosc, J.; Frye, J.; Montagne, L.; Amoureux, J.-P.; Pruski, M. SPAM-MQ-HETCOR: An Improved Method for Heteronuclear Correlation Spectroscopy between Quadrupolar and Spin-1/2 Nuclei in Solid-State NMR. *Phys. Chem. Chem. Phys.* **2006**, *8* (1), 144−150.

(26) Amoureux, J. P.; Trebosc, J.; Wiench, J.; Pruski, M. HMQC and Refocused-INEPT Experiments Involving Half-Integer Quadrupolar Nuclei in Solids. *J. Magn. Reson.* **2007**, *184* (1), 1−14.

(27) Siegel, R.; Rocha, J.; Mafra, L. Combining STMAS and CRAMPS NMR Spectroscopy: High-Resolution HETCOR NMR Spectra of Quadrupolar and 1H Nuclei in Solids. *Chem. Phys. Lett.* **2009**, *470* (4−6), 337−341.

(28) Morais, C. M.; Montouillout, V.; Deschamps, M.; Iuga, D.; Fayon, F.; Paz, F. A. A.; Rocha, J.; Fernandez, C.; Massiot, D. 1D to 3D NMR Study of Microporous Alumino-Phosphate AlPO4−40. *Magn. Reson. Chem.* **2009**, *47* (11), 942−947.

(29) Trébosc, J.; Lafon, O.; Hu, B.; Amoureux, J.-P. Indirect High-Resolution Detection for Quadrupolar Spin-3/2 Nuclei in Dipolar HMQC Solid-State NMR Experiments. *Chem. Phys. Lett.* **2010**, *496* (1−3), 201−207.

(30) Martineau, C.; Bouchevreau, B.; Taulelle, F.; Trébosc, J.; Lafon, O.; Amoureux, J. P. High-Resolution through-Space Correlations between Spin-1/2 and Half-Integer Quadrupolar Nuclei Using the MQ-D-R-INEPT NMR Experiment. *Phys. Chem. Chem. Phys.* **2012**, *14* (19), 7112.

(31) Gan, Z.; Gor'kov, P. L.; Brey, W. W.; Sideris, P. J.; Grey, C. P. Enhancing MQMAS of Low-Gamma Nuclei by Using a High B-1 Field Balanced Probe Circuit. *J. Magn. Reson.* **2009**, *200* (1), 2−5.

(32) Hildebrand, M.; Hamaed, H.; Namespetra, A. M.; Donohue, J. M.; Fu, R.; Hung, I.; Gan, Z.; Schurko, R. W. 35Cl Solid-State NMR of HCl Salts of Active Pharmaceutical Ingredients: Structural Prediction, Spectral Fingerprinting and Polymorph Recognition. *CrystEngComm* **2014**, *16* (31), 7334−7356.
(33) Namespetra, A. M.; Hirsh, D. A.; Hildebrand, M. P.; Sandre, A. R.; Hamaed, H.; Rawson, J. M.; Schurko, R. W. 35Cl Solid-State NMR Spectroscopy of HCl Pharmaceuticals and Their Polymorphs in Bulk and Dosage Forms. *CrystEngComm* **2016**, *18* (33), 6213−6232.
(34) Horter, D.; Dressman, J. B. Influence of Physicochemical Properties on Dissolution of Drugs in the Gastrointestinal Tract. *Adv. Drug Delivery Rev.* **2001**, *46* (1−3), 75−87.
(35) Bauer, J.; Morley, J.; Spanton, S.; Leusen, F. J. J.; Henry, R.; Hollis, S.; Heitmann, W.; Mannino, A.; Quick, J.; Dziki, W. Identification, Preparation, and Characterization of Several Polymorphs and Solvates of Terazosin Hydrochloride. *J. Pharm. Sci.* **2006**, *95* (4), 917−928.
(36) van Eck, E. R. H.; Janssen, R.; Maas, W. E. J. R.; Veeman, W. S. A Novel Application of Nuclear Spin-Echo Double-Resonance to Aluminophosphates and Aluminosilicates. *Chem. Phys. Lett.* **1990**, *174* (5), 428−432.
(37) Grey, C. P.; Veeman, W. S.; Vega, A. J. Rotational Echo 14N/13C/1H Triple Resonance Solid-state Nuclear Magnetic Resonance: A Probe of 13C−14N Internuclear Distances. *J. Chem. Phys.* **1993**, *98* (10), 7711−7724.
(38) Grey, C. P.; Vega, A. J. Determination of the Quadrupole Coupling-Constant of the Invisible Aluminum Spins in Zeolite HY with 1H/27Al TRAPDOR NMR. *J. Am. Chem. Soc.* **1995**, *117* (31), 8232−8242.
(39) Jarvis, J. A.; Haies, I. M.; Williamson, P. T. F.; Carravetta, M. An Efficient NMR Method for the Characterisation of 14N Sites through Indirect 13C Detection. *Phys. Chem. Chem. Phys.* **2013**, *15* (20), 7613.
(40) Hung, I.; Gor'kov, P.; Gan, Z. Efficient and Sideband-Free 1H-Detected 14N Magic-Angle Spinning NMR. *J. Chem. Phys.* **2019**, *151* (15), 154202.
(41) Bak, M.; Rasmussen, J. T.; Nielsen, N. C. SIMPSON: A General Simulation Program for Solid-State NMR Spectroscopy. *J. Magn. Reson.* **2000**, *147* (2), 296−330.
(42) Bodenhausen, G.; Kogler, H.; Ernst, R. R. Selection of Coherence-Transfer Pathways in NMR Pulse Experiments. *J. Magn. Reson.* **1984**, *58* (3), 370−388.
(43) Bain, A. D. Coherence Levels and Coherence Pathways in NMR. A Simple Way to Design Phase Cycling Procedures. *J. Magn. Reson.* **1984**, *56* (3), 418−427.
(44) Gan, Z. H. Satellite Transition Magic-Angle Spinning Nuclear Magnetic Resonance Spectroscopy of Half-Integer Quadrupolar Nuclei. *J. Chem. Phys.* **2001**, *114* (24), 10845−10853.
(45) Amoureux, J. P.; Huguenard, C.; Engelke, F.; Taulelle, F. Unified Representation of MQMAS and STMAS NMR of Half-Integer Quadrupolar Nuclei. *Chem. Phys. Lett.* **2002**, *356* (5−6), 497−504.
(46) Hung, I.; Trebosc, J.; Hoatson, G. L.; Vold, R. L.; Amoureux, J. P.; Gan, Z. Q-Shear Transformation for MQMAS and STMAS NMR Spectra. *J. Magn. Reson.* **2009**, *201* (1), 81−86.

https://dx.doi.org/10.1021/acs.jpclett.0c01236
J. Phys. Chem. Lett. 2020, 11, 4734−4740